Electronic Supplementary Material (ESI) for Sustainable Energy & Fuels.

Supporting Information

One-step construction of Co_2P nanoparticles encapsulated in N, P co-doped biomass-based porous carbon as bifunctional efficient electrocatalysts for overall water splitting

Di Li[a], Zengyong Li[a], Jiaojiao Ma[a], Xinwen Peng*[a] and Chuanfu Liu*[a]

* Corresponding authors (chfliu@scut.edu.cn, fexwpeng@scut.edu.cn)

[a] State Key Laboratory of Pulp and Paper Engineering, School of Light Industry and Engineering, South China University of Technology, 381 Wushan Road, Guangzhou 510641, P. R. China

Electrode preparation and electrochemical measurement

All electrochemical tests were conducted with a standard three-electrode system at the electrochemical workstation. A graphite rod and saturated calomel electrode (SCE) were used as the counter and reference electrode, respectively. All potentials were referenced to the reversible hydrogen electrode (RHE) by the equation $E_{RHE}=E_{(SCE)}$ + 0.0591 pH + 0.241. Typically, 2.5 mg of the catalyst powders was dispersed in 480 μL of a 3:1 v/v water/ethanol mixed solvents along with 20 μL of Nafion solution, and the mixture was sonicated for about 45 min to generate a homogeneous catalyst ink. Then, 5 μL of the catalyst ink was drop-casting onto a polished glass carbon electrode, leading to a catalyst loading of 0.35 mg cm^{-2}. Polarization curves were acquired by sweeping the potential from 0 to -0.8 V (vs SCE) at a potential sweep rate of 5 mV/s. Accelerated stability tests were performed in 0.5 M H_2SO_4 at room temperature by potential cycling between 0 to -0.8 V (vs SCE) at a potential sweep rate of 100 mV/s for a given number of cycles. The pH durability of catalyst was processed in different electrolyte media (0.5 M H_2SO_4, 1 M KOH). In all measurements, the SCE reference electrode was calibrated with respect to a reversible hydrogen electrode (RHE). The electrochemical impedance spectroscopy (EIS) was carried out in the range from 10^5 to 0.01 Hz. All the experiments were processed at room temperature. The OER activities were measured by linear sweep voltammetry (LSV) method with a scan rate of 5 mV s^{-1} at room temperature in 1 M KOH solution. The stability measurements were tested by cyclic voltammetry scanning 1000 cycles (CV, sweep rate, 100 mV s^{-1}) and long-term chronoamperometry method. EIS was

carried out in the range from 10^5 to 0.01 Hz. The electrochemically surface area (ECSA) also was investigated by CV to determine the electrochemical double-layer capacitances (C_{dl}). For overall-water splitting studies, the full electrolyze configuration was assembled using Co_2P@NPPC loaded on a carbon cloth as a two-electrode with the catalyst loading of 1.25 mg cm^{-2}.

DFT calculations

The VASP program[1-2] was used for calculations. PBE functional[3] was employed, and the ENCUT parameter was set to 500 eV. The reciprocal space was sampled with Gamma point. Both lattice parameters and atom positions were fully optimized for each structure.[4] The Grimme's D3BJ correction[5] was employed to take account of dispersion interaction.

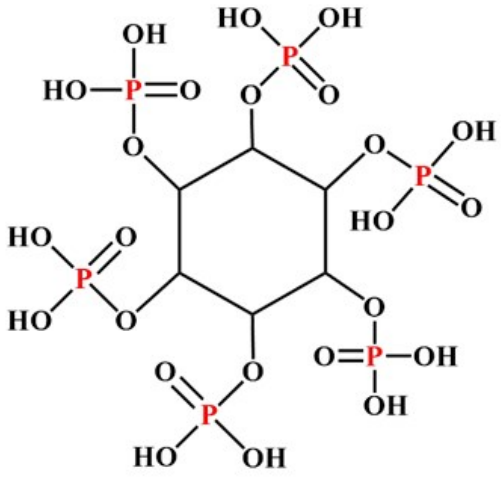

Fig. S1. Molecular structure of PA.

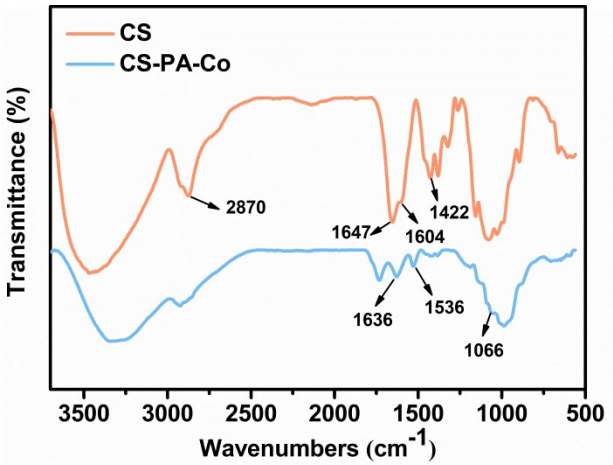

Fig. S2. FTIR spectra of CS and CS-PA-Co, respectively.

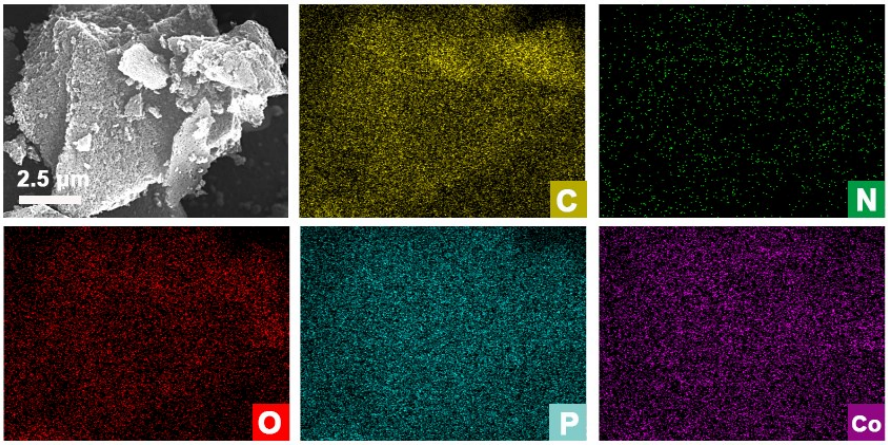

Fig. S3. Surface characterization of Co_2P@NPPC. SEM image, and the corresponding EDS element mappings of C, N, O, P and Co.

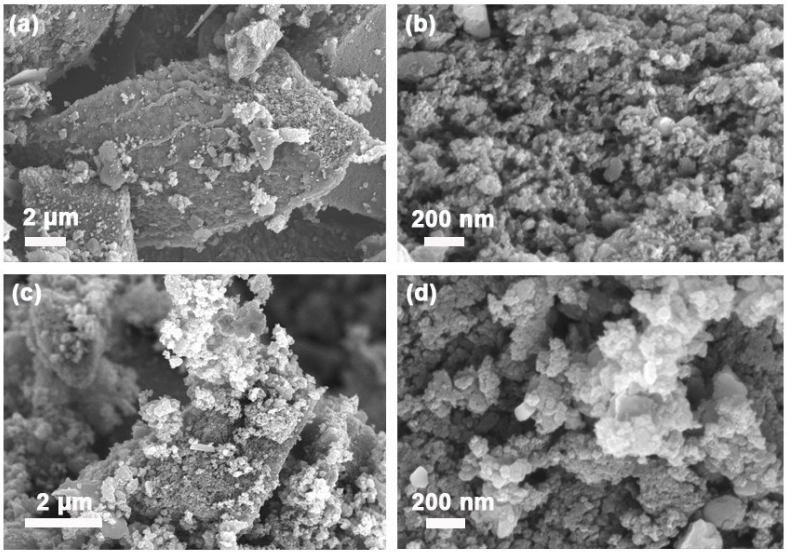

Fig. S4. SEM images of $Co(PO_3)_2$@NPPC-700 (a, b) and $Co(PO_3)_2$@NPPC-800 (c, d)

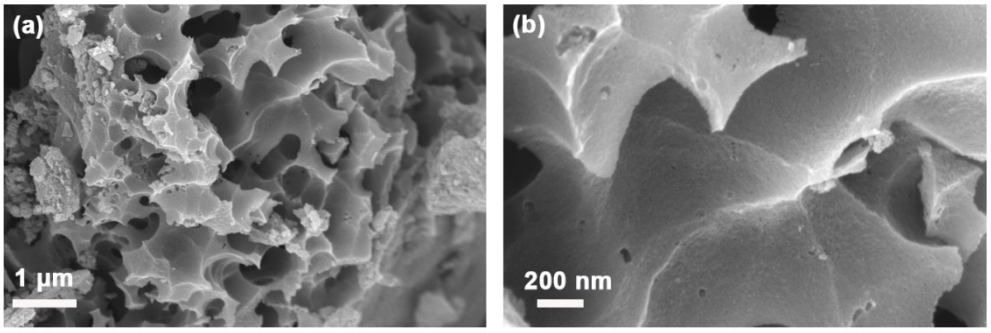

Fig. S5. Morphology and structure of the Co@NPC

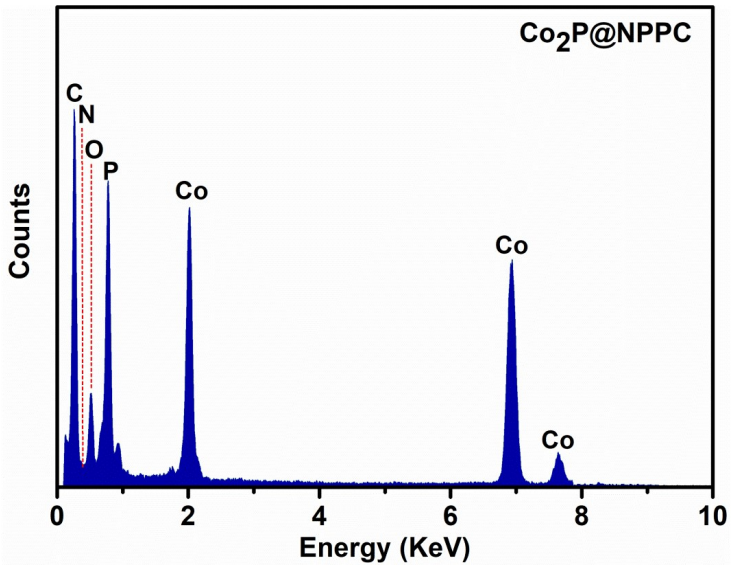

Fig. S6. EDX spectrum of the Co_2P@NPPC

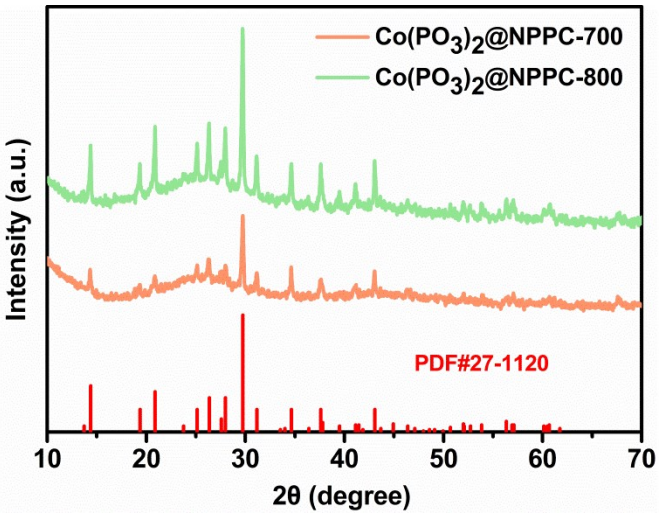

Fig. S7. X-ray diffraction (XRD) spectra of $Co(PO_3)_2$@NPPC-700 and $Co(PO_3)_2$@NPPC-800

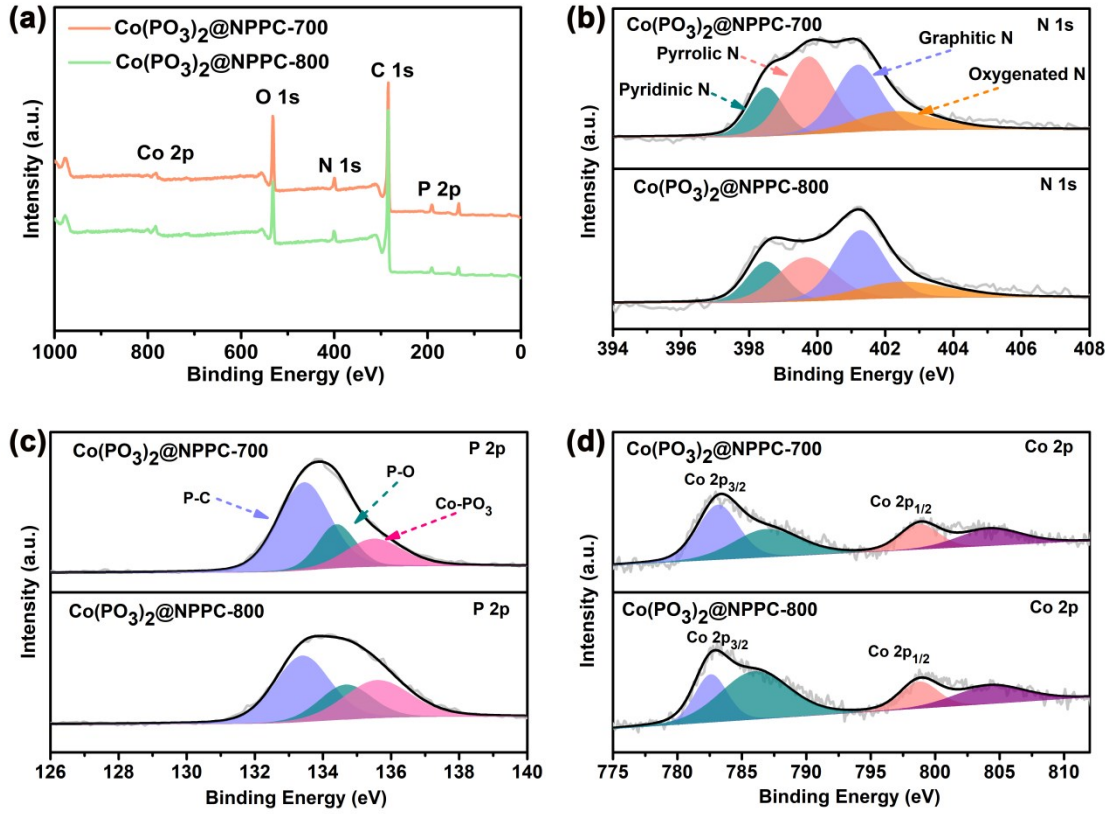

Fig. S8. (a) XPS survey spectrum, and (b-d) the high resolution XPS spectra of $Co(PO_3)_2$@NPPC-700 and $Co(PO_3)_2$@NPPC-800.

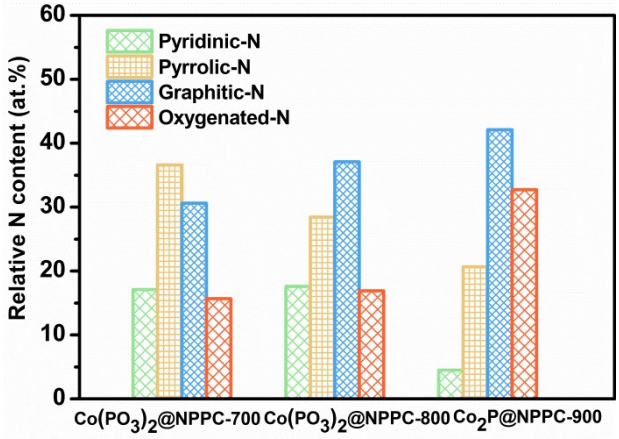

Fig. S9. The content of different N species in $Co(PO_3)_2$@NPPC-700, $Co(PO_3)_2$@NPPC-800 and Co_2P@NPPC-900.

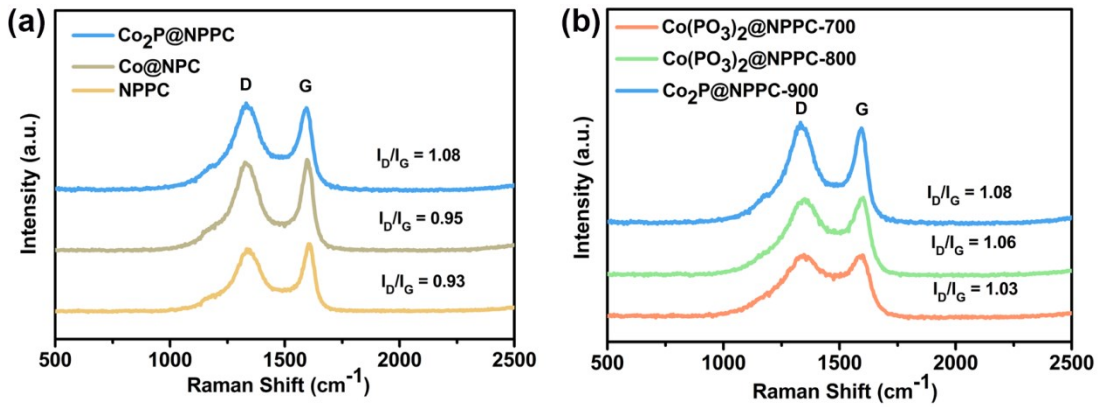

Fig. S10. Raman spectra of Co_2P@NPPC, Co@NPC and NPPC (a), and samples pyrolyzed at different temperatures (b).

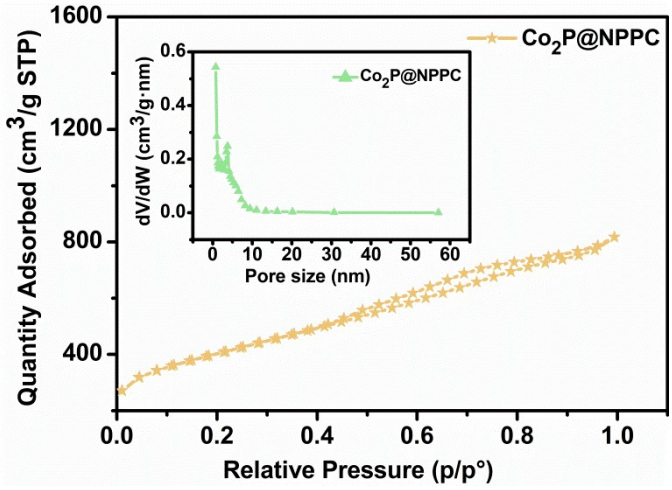

Fig. S11. N_2 adsorption−desorption isotherms of Co_2P@NPPC and inset is the distributions of pores of Co_2P@NPPC.

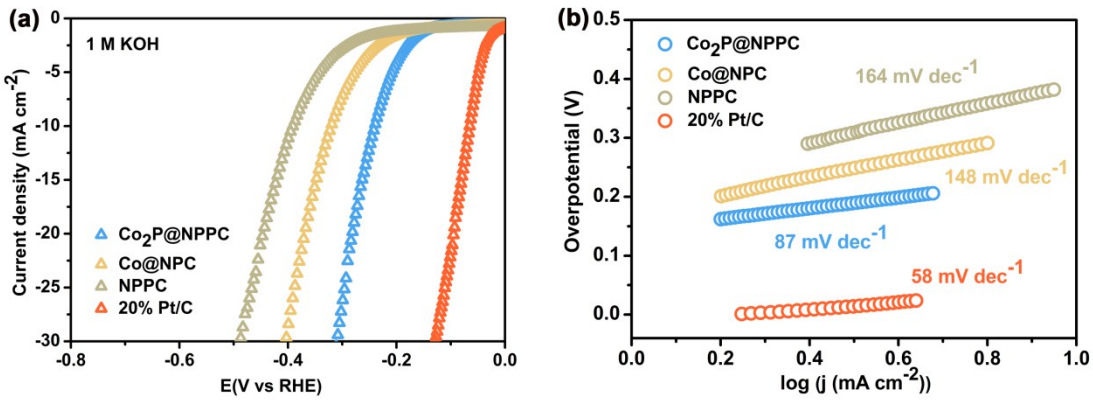

Fig. S12. (a) HER polarization curves of Co_2P@NPPC, Co@NPC, NPPC and Pt/C in 1 M KOH. (b) The corresponding Tafel slopes of all samples.

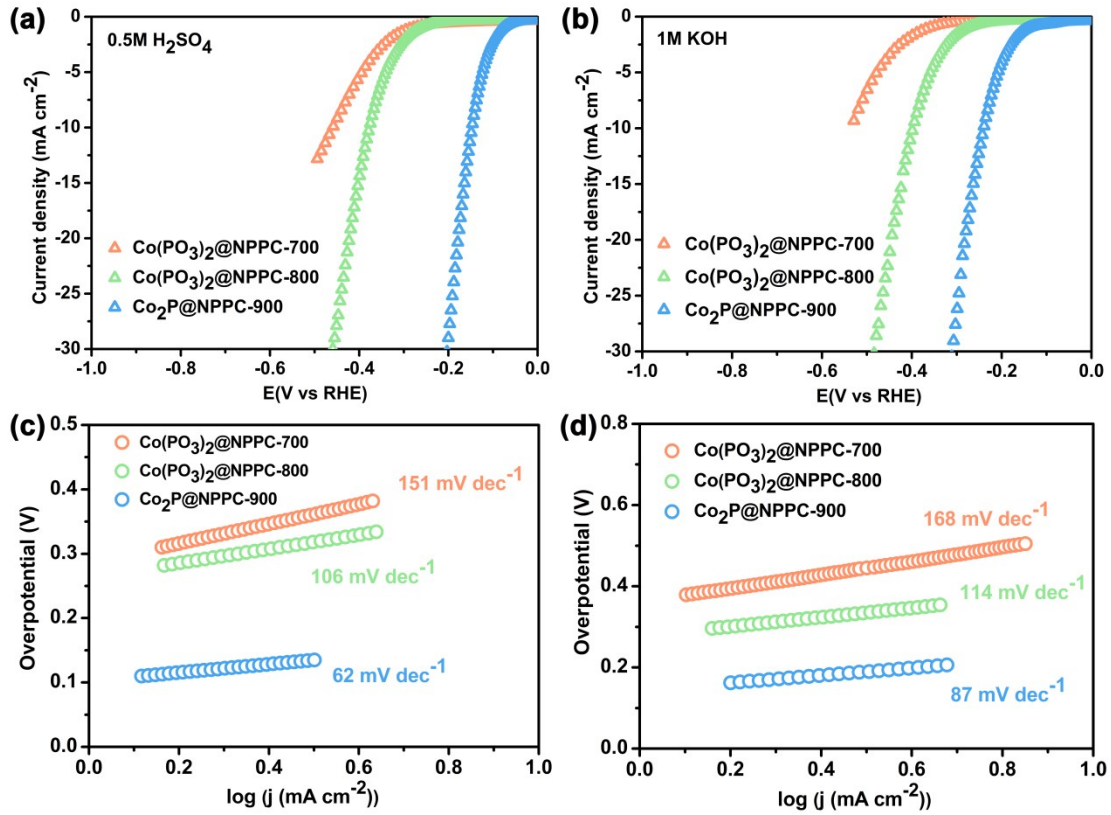

Fig. S13. (a, b) HER polarization curves and (c, d) the corresponding Tafel plots of Co_2P@NPPC-900, and the compared samples in 0.5 M H_2SO_4 and 1 M KOH with a scan rate of 5 mV s^{-1} at room temperature, respectively.

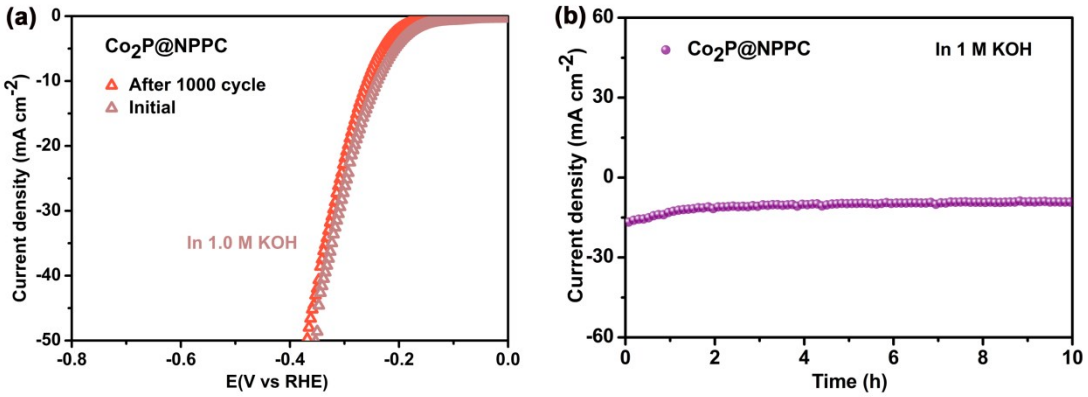

Fig. S14. (a) HER polarization curves of Co_2P@NPPC before and after 1000 cycles of CV and (b) the insets are the chronoamperometric curves in 1 M KOH.

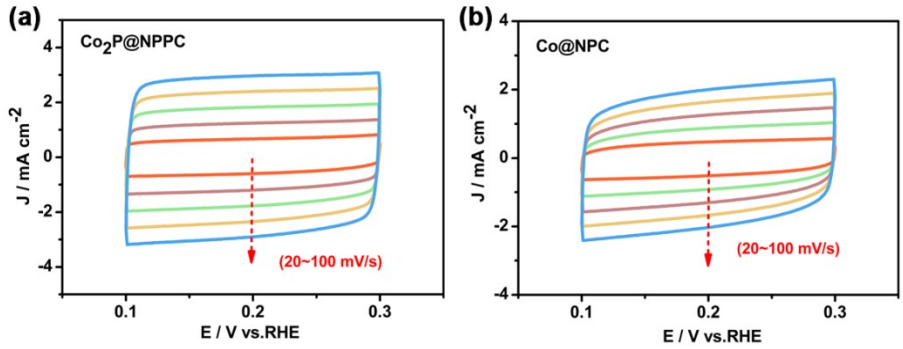

Fig. S15. (a, b) CV curves of Co_2P@NPPC and Co@NPC at different scan rates.

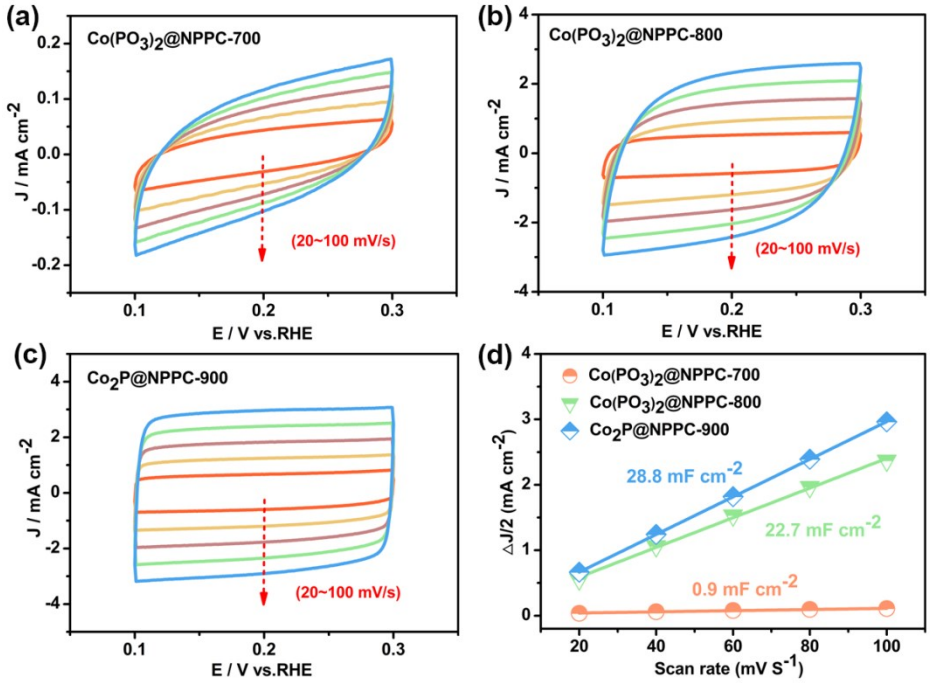

Fig. S16. (a-c) CV curves of Co_2P@NPPC and the compared samples pyrolyzed at different temperatures, and (d) the variation of double layer charging currents as a function of scan rate.

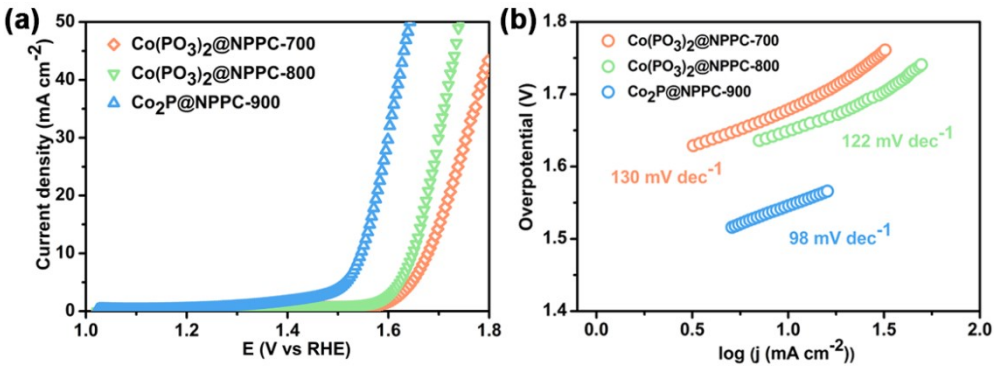

Fig. S17. (a) OER polarization curves and (b) the corresponding overpotentials at j = 10 mA cm^{-2} in 1 M KOH of Co_2P@NPPC, and the compared samples pyrolyzed at different temperatures.

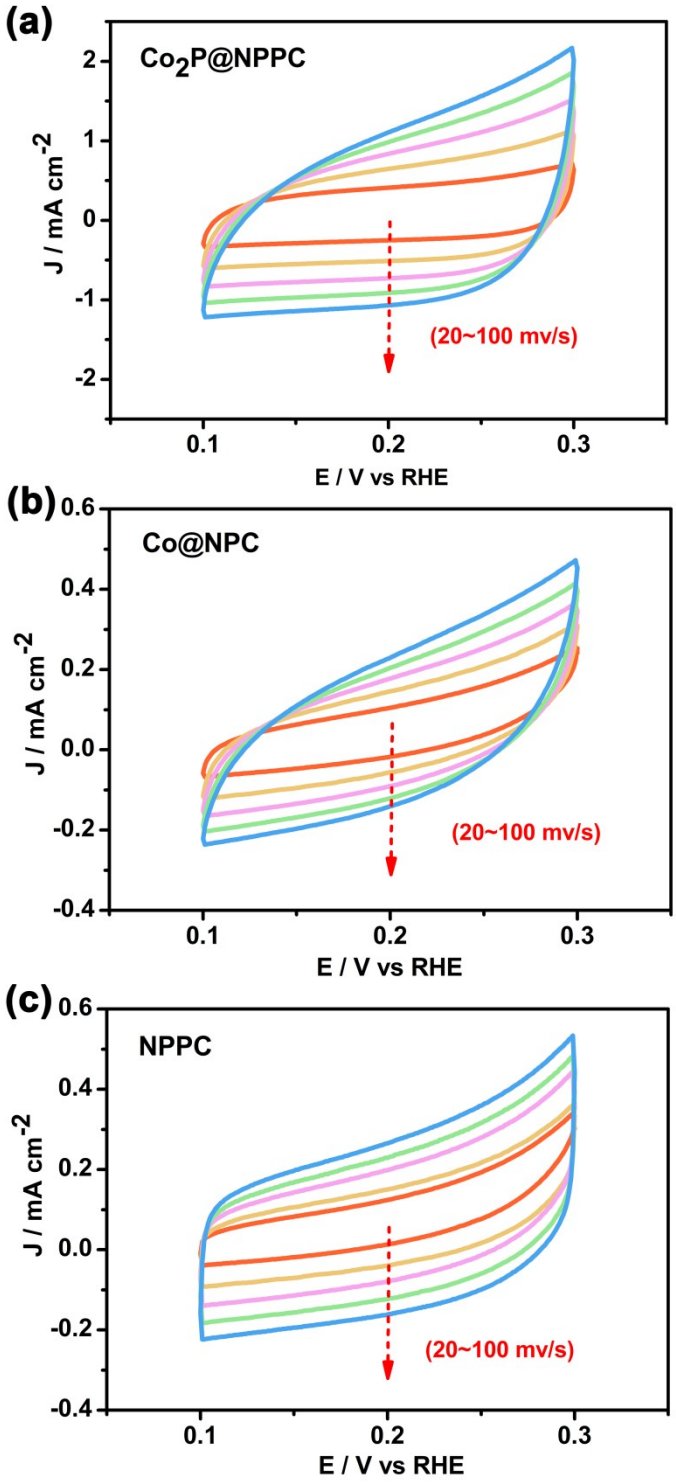

Fig. S18. CV curves of (a) Co_2P@NPPC , (b) Co@NPC and (c) NPPC at different scan rates.

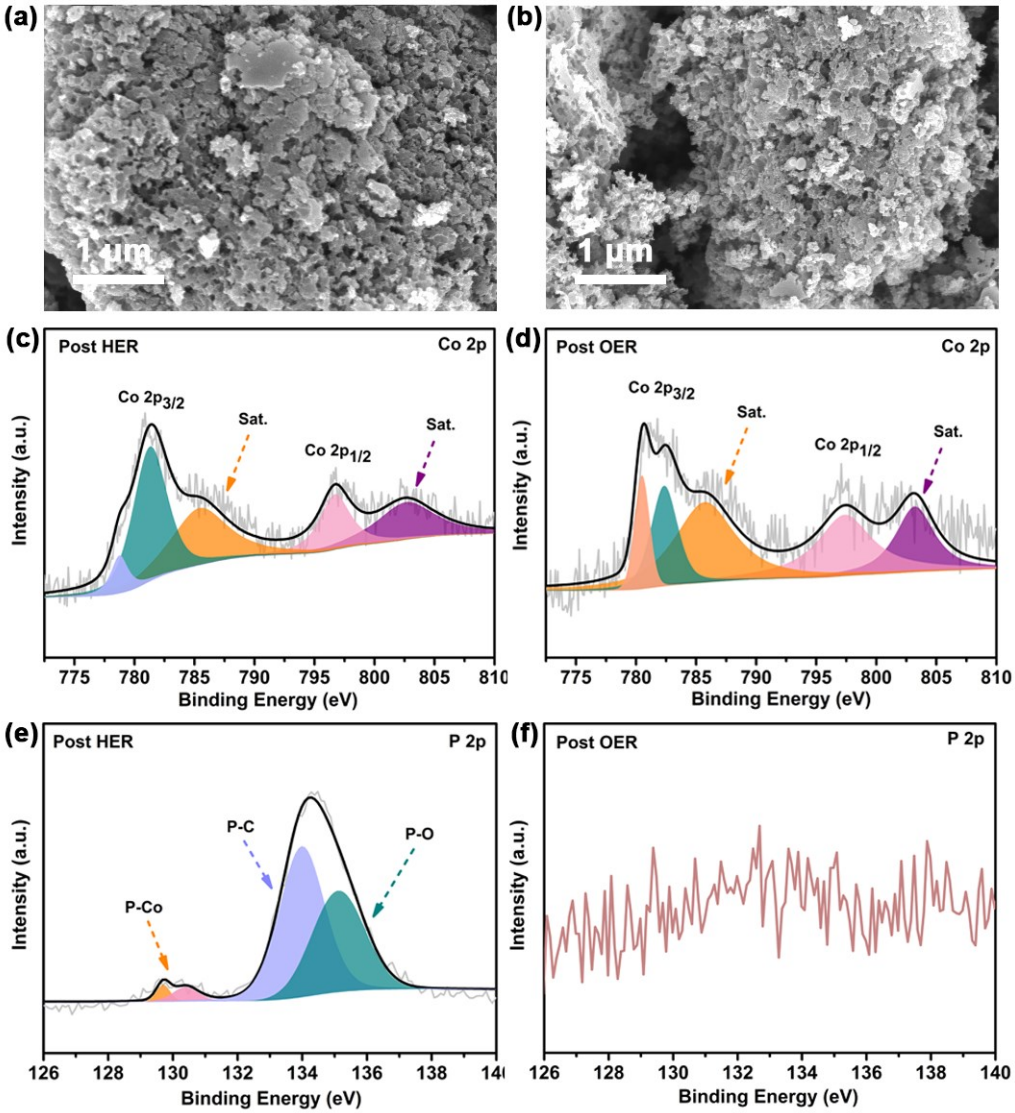

Fig. S19. (a, b) SEM images of Co_2P@NPPC after HER and OER test, respectively. High-resolution scans of (c, d) Co 2p and (e, f) P 2p spectra after HER and OER test.

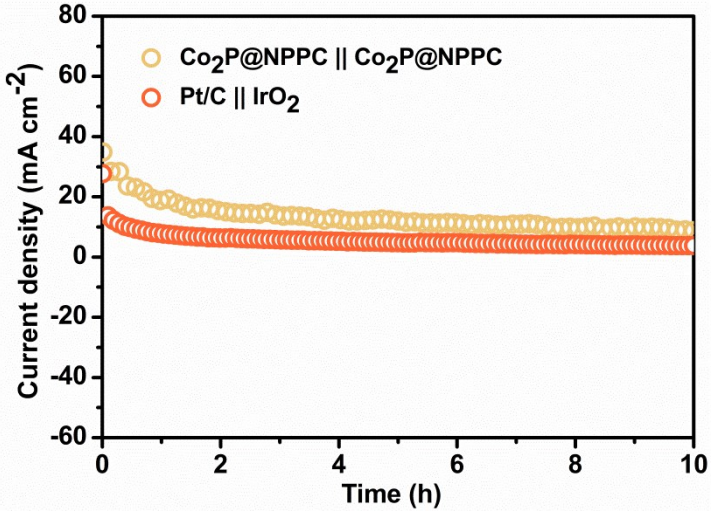

Fig. S20. Chronopotentiometric curve of water electrolysis in 1 M KOH.

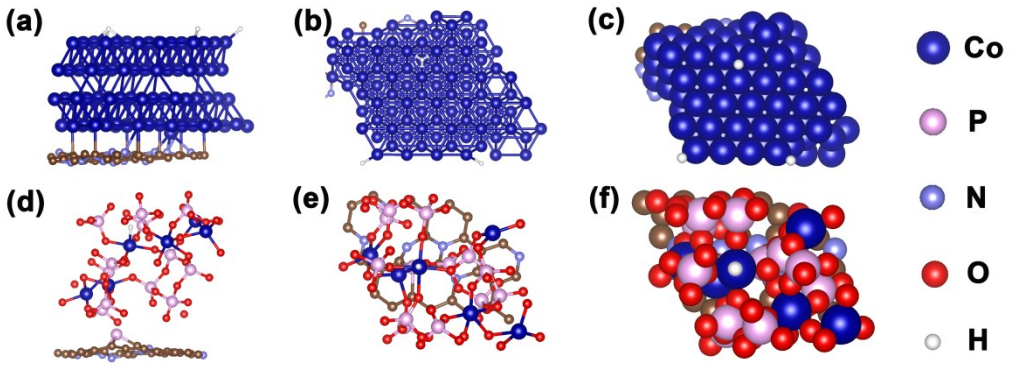

Fig. S21. Side view and top view of the models of Co@NPC (a, b and c) and $Co(PO_3)_2$@NPPC (d, e and f) of the optimized structure of H adsorption on Co and $Co(PO_3)_2$@NPPC surface, respectively.

Table S1. XPS elemental analysis of Co_2P@NPPC and $Co(PO_3)_2$@NPPC samples.

Samples	$Co(PO_3)_2$@NPPC-700	$Co(PO_3)_2$@NPPC-800	Co_2P@NPPC-900
C (at%)	73.23	79.7	88.21
N (at%)	4.54	3.87	1.73
O (at%)	17.24	12.68	7.34
P (at%)	4.27	2.99	1.68
Co (at%)	0.71	0.75	1.03

Table S2. The BET surface areas, BJH pore volume and Pore size of Co_2P@NPPC

Samples	BET surface areas (m^2/g)	Pore volume (cm^3/g)	Pore size (nm)
Co_2P@NPPC	1380	1.18	3.44

Table S3. Comparision of HER performance in 0.5 M H_2SO_4 solution for Co_2P@NPPC with other non-noble metal electrocatalysts.

Catalyst	Voltage@10mA cm^{-2} (mV)	Tafel slope ($mV\ dec^{-1}$)	Reference
Co_2P@NPPC	147	62	This work
$Ni_{0.62}Co_{0.38}P$	166	72	*Adv. Funct. Mater.* **2016,** *26*, 7644-7651
MoP NSs/CFs	200	56	*Appl. Catal. B* **2015,** *164*, 144-150
Co_9S_8@MoS_2/CNFs	190	110	*Adv. Mater.* **2015,** *27*, 4752-4759
$Fe_{0.43}Co_{0.57}S_2$	220	56	*Energy Environ. Sci.* **2013,** *6*, 3553-3558
FeP	250	67	*Chem. Commun.* **2013,** *49*, 6656-6658
Co@NC	210	108	*J. Mater. Chem. A* **2014,** *2*, 20067-20074
Co@NC/NG	180	79	*Chem. Mater.* **2015,** *27*, 2026-2032
NG/Co-doped C	229	126	*Adv. Funct. Mater.* **2015,** *25*, 872-882
Au@Zn-Fe-C	123	78.2	*ACS Catal.* **2016,** *6*, 1045-1053
WP_2	161	57	*ACS Catal.* **2015,** *5*, 145-149
Ni-Co-P nanocube	150	60.6	*Chem. Commun*. **2016**, 52, 1633-1636
Ni-Co-MoS_2	155	51	*Adv. Mater*. **2016**, 28, 9006-9011
MoP@PC	153	66	*Angew. Chem. Int. Ed*. **2016**, 55, 12854-12858
Fe doped NiS_2	198	42	*J. Mater. Chem. A* **2019**, 7, 4971-4976
CoP@NG	158	63.8	*Electrochim. Acta* **2019**, 307, 543-552
CoP hollow polyhedra	159	59	*ACS Appl. Mater. Interfaces* **2016**, 8, 2158-2165
2D Co_2P	41	35	*Nanoscale,* **2018**,10, 6844-

			6849

Table S4. Comparision of HER performance in 1 M KOH solution for Co_2P@NPPC with other non-noble metal electrocatalysts.

Catalyst	Voltage@10mA cm^{-2} (mV)	Tafel slope (mV dec^{-1})	Reference
Co_2P@NPPC	240	87	This work
CoP/CC	209	129	*J. Am. Chem. Soc.* **2014,** *136*, 7587-7590
CoOx@CN	232	115	*J. Am. Chem. Soc.* **2015,** *137*, 2688-2694
NiCoP/rGO	209	124.1	*Adv. Funct. Mater.* **2016,** *26*, 6785-6796
Co_9S_8@C	250	-	*ACS Appl. Mater. Interfaces* **2015,** *7*, 980-988
Mo_2C	270	78	*J. Am. Chem. Soc.* **2015,** *137*, 7035-7038
Co-NRCNTs	370	-	*Angew. Chem. Int. Ed.* **2014,** *53*, 4372-4376
CoO_x@CN	232	115	*J. Am. Chem. Soc.* **2015**, 137, 2688-2694.
Ni/Mo_2C-PC	179	101	*Chem. Sci.* **2017,** *8*, 968-973
Co-PCNFs	249	92	*J. Mater. Chem. A* **2016,** *4*, 12818-12824
MnNi	360	-	*Adv. Funct. Mater.* **2015,** *25*, 393-399
FeP	218	146	*ACS Catal.* **2014,** *4*, 4065-4069
Pt-Co_2P	2	44	*Energy Environ. Sci.* **2020**, 13, 3110-3118

Table S5. Comparision of OER performance in 1 M KOH solution for Co_2P@NPPC with other non-noble metal electrocatalysts.

Catalyst	Voltage@10mA cm^{-2} (mV)	Tafel slope (mV dec^{-1})	Reference
Co_2P@NPPC	316	98	This work
NiCoP	340	86	*Adv. Mater. Interfaces* **2016,** *3*, 1500454
PNC@Co	370	76	*J. Mater. Chem. A* **2016,** *4*, 3204-3209.
CoO_x@CN	385	-	*J. Am. Chem. Soc.* **2015,** *137*, 2688-2694
CoP NPs/C	340	99	*ACS Catal.* **2015,** *5*, 6874-6878
Co_3O_4@C/CP	370	82	*Nano Energy* **2016,** *25*, 42-50
$CoFeO_x$ film	360	-	*J. Am. Chem. Soc.* **2013,** *135*, 16977-16987
Co_9S_8@MoS_2/CNFs	430	61	*Adv. Mater.* **2015,** *27*, 4752-4759
C-Co NPs	390	-	*J. Am. Chem. Soc.* **2015,** *137*, 7071-7074
Co-P film	345	47	*Angew. Chem. Int. Ed.* **2015,** *54*, 6251-6254
CoP-MNA/Ni Foam	390	65	*Adv. Funct. Mater.* **2015,** *25*, 7337-7347
Co-P@NC-800	370	79	*ACS Appl. Mater. Interfaces* **2017**, 9, 40171-40179
NiCoP/C nanoboxes	330	96	*Angew. Chem. Int. Ed*. **2017**, 56, 3897-3900
Co-C_3N_4/CNT	380	68.4	*J. Am. Chem. Soc*. **2017**, 139, 3336-3339
Co-P/NC	354	52	*Chem. Mater.* **2015**, 27, 7636-7642
Mo_2C@CS	380	98	*ChemSusChem* **2017**, 10, 3540-3546
Co_3O_4@BP	400	63	*ACS Appl. Mater. Interfaces* **2019**, 11, 17459-17466
Co_2P@NC-Fe_2P	260	41	*ACS Appl. Mater. Interfaces* **2020**, 12, 25884−25894
Co/P/N-CNP-5/NF	311	67.7	*Electrochim. Acta* **2020**, 337,

			135807
CoO/Co_xP	370	101	*J. Mater. Chem. A* **2020,** 8, 9177-9184.

Table S6. Comparison with various electrocatalysts for overall water splitting in 1 M KOH solution

Catalyst	Voltage@10mA cm^{-2} (V)	Reference
Co_2P@NPPC	1.65	This work
Co_3O_4 crystals	1.91	*Chem. Commun.* **2015,** *51*, 8066-8069
Co-S sheets	1.743	*ACS Nano* **2016,** *10*, 2342-2348
Ni_3S_2	1.76	*J. Am. Chem. Soc.* **2015,** *137*, 14023-14026
CoP/rGO	1.7	*Chem. Sci.* **2016,** *7*, 1690-1695
Ni_5P_4	~1.7	*Angew. Chem. Int. Ed.* **2015,** *54*, 12361-12365
Co_2B	1.81	*Adv. Energy Mater.* **2016,** *6*, 1502313
$Co_{24}Ni_1B_{75}$@NF	1.72	*J. Mater. Chem. A* **2017,** *5*, 12379-12384
Ni_xCo_3-xO_4 ||NiCo/$NiCoO_x$	1.75	*ACS Appl. Mater. Interfaces* **2016,** *8*, 3208-3214
$CoTe_2$@NCNTFs	1.67	*J. Mater. Chem. A* **2018**, 6, 3684-3691
Mo_2C@CS	1.73	*ChemSusChem* **2017**, 10, 3540-3546
Co-P/NC	~1.71	*Chem. Mater.* **2015**, 27, 7636-7642
EG/$Co_{0.85}Se$/NiFe-LDH	1.67	*Energy Environ. Sci*. **2016**, 9, 478-483
$NiCo_2S_4$ NA	1.68	*Nanoscale* **2015**, 7, 15122-15126
CoO/MoO_x	1.72	*ACS Sustainable Chem. Eng.* **2016**, 4, 3743-3749
Ni_5P_4 film	~1.69	*Angew. Chem. Int. Ed*. **2015**, 54, 12361-12365
$Cr_{0.2}Co_{1.8}P$/CB	1.63	*ACS Appl. Mater. Interfaces* **2020**, 12, 47397−47407
BP/Co_2P	1.92	*Angew. Chem. Int. Ed*. **2018**, 57, 2600-2604
CoP-Co_2P@PC	1.57	*Small* **2019**, 15, 1804546

Reference

(1) G. Kresse; Furthmiiller, J. Efficiency of ab-initio total energy calculations for metals and semiconductors using a plane-wave basis set. *Comput. Mater. Sci.* **1996,** *6*, 15-50.

(2) G. Kresse; Furthmiiller, J. Efficient iterative schemes for ab initio total-energy calculations using a plane-wave basis set. *Phys. Rev. B: Condens. Matter* **1996,** *54*, 11169-11186.

(3) John P. Perdew; Kieron Burke; Ernzerhof, M. Generalized Gradient Approximation Made Simple. *Phys. Rev. Lett.* **1996,** *77*, 3865-3868.

(4) Kong, F.; Longo, R. C.; Yeon, D.-H.; Yoon, J.; Park, J.-H.; Liang, C.; Kc, S.; Zheng, Y.; Doo, S.-G.; Cho, K. Multivalent Li-Site Doping of Mn Oxides for Li-Ion Batteries. *J. Phys. Chem. C* **2015,** *119*, 21904-21912.

(5) Stefan Grimme; Jens Antony; Stephan Ehrlich; Krieg, H. A consistent and accurate ab initio parametrization of density functional dispersion correction (DFT-D) for the 94 elements H-Pu. *J. Chem. Phys.* **2010,** *132*, 154104.